ADVANCED MATERIALS
www.advmat.de

Materials Views
www.MaterialsViews.com

Intrinsic Topological Insulator Bi_2Te_3 Thin Films on Si and Their Thickness Limit

By *Yao-Yi Li, Guang Wang, Xie-Gang Zhu, Min-Hao Liu, Cun Ye, Xi Chen, Ya-Yu Wang, Ke He, Li-Li Wang, Xu-Cun Ma, Hai-Jun Zhang, Xi Dai, Zhong Fang, Xin-Cheng Xie, Ying Liu, Xiao-Liang Qi, Jin-Feng Jia,* Shou-Cheng Zhang,* and *Qi-Kun Xue*

Layer-by-layer molecular beam epitaxy growth of high quality Bi_2Te_3 films has been achieved on Si(111) substrate. The Te-rich growth dynamics is found crucial for high quality stoichiometric Bi_2Te_3 with few defects. *In situ* angle resolved photoemission spectroscopy (ARPES) measurement reveals that the as-grown Bi_2Te_3 films without any doping are an intrinsic topological insulator with its Fermi level intersecting only the metallic surface states, which is different from available bulk crystal of Bi_2Te_3. Experimentally, we find that the single-Dirac-cone surface state develops at a thickness of two quintuple layers (2 QL). Theoretically, we show that the interaction between the surface states from both sides of the film, which is determined by the penetration depth of the topological surface state wavefunctions, sets this lower thickness limit. The success in growing high quality films by state-of-art molecular beam epitaxy technique opens a new avenue for engineering of topological materials based on well-developed Si technology, and is of significant importance for potential applications of topological insulators.

Traditionally, Bi_2Te_3 is known for having the highest figure-of-merit coefficient $ZT \approx 1$ among bulk thermoelectric materials.[1–3] Recent theory and experiment reveal that stoichiometric Bi_2Te_3 is also a topological insulator (TI) with time-reversal-symmetry protected surface states that reside in its bulk insulating gap.[4–6] The metallic surface states consist of a single Dirac cone at the Γ point and are predicted to exhibit a number of striking electromagnetic properties,[7–11] which have recently attracted great attention.[4–20] Experimentally, angle-resolved photoemission spectroscopy (ARPES) is the only direct way to determine if a sample is a TI by mapping the band structure and see if the Fermi level (E_F) only intersects the metallic surface state.[5,6,11,16,17] However, the reported topological insulators such as bulk Bi_2Te_3 and Bi_2Se_3 all suffer from a great amount of unwanted bulk carriers,[5,6,11,16–19] and an intense bulk electron pocket appears at the Fermi level due to the presence of vacancies and anti-site defects.[5,6,11] With the bulk electronic states at E_F, it is difficult to characterize the pristine topological transport property and to use them to develop topological devices that rely only on the behaviors of Dirac fermions. Therefore, a major obstacle in the rapidly developing field of TIs is the extreme difficulty in growing intrinsic TI materials. Here we define intrinsic by reference to intrinsic semiconductors: its Fermi level lies in between the bulk conduction band minimum (CBM) and the bulk valence band maximum (VBM) and only intersects the metallic surface state.

The Bi_2Te_3 crystals studied in recent experiments were grown by melting stoichiometric mixture of Bi and Te in a crucible.[5,6,11] Local composition fluctuation, which results in a high background carrier density,[5,6] cannot be avoided with this technique. To compensate the background carriers and remove the bulk states from the Fermi level, the materials had to be heavily doped by 0.67% Sn.[5] The situation makes systematic doping control and device gating difficult. Thin films have several advantages: band engineering can be achieved by bipolar or gradient doping, and tunneling junctions, as well as heterostructures and superlattices. Growth of Bi_2Te_3 and Bi_2Se_3 films by molecular beam epitaxy (MBE) and other techniques has been investigated previously.[21–23] With these methods, nominally stoichiometric single crystalline films could easily be prepared. However, discussion of their topological properties was not possible in those studies since the band structure of the films is unknown. So, it's difficult to judge that the quality of the films is better than that of bulk counterpart and they are the topological insulator without doping.

The main purpose of this work is to establish the MBE growth conditions by which intrinsic topological insulator thin films of Bi_2Te_3 can be readily obtained. We do this by a systematic study of growth dynamics under various Te_2/Bi flux ratios and Si substrate temperatures with reflection high-energy electron diffraction (RHEED). We identify unique Te-rich growth dynamics for preparing intrinsic topological insulator films by the characteristic RHEED intensity oscillations of layer-by-layer MBE growth. The high quality of the grown films is also confirmed by *in situ* scanning tunneling microscopy (STM). Remarkably, our *in situ*

[*] Y.-Y. Li, G. Wang, X.-G. Zhu, M.-H. Liu, C. Ye, Prof. X. Chen, Prof. Y.-Y. Wang, Prof. J.-F. Jia, Prof. Q.-K. Xue
Key Lab for Atomic, Molecular and Nanoscience
Department of Physics
Tsinghua University
Beijing, 100084 (P. R. China)
E-mail: jjf@mail.tsinghua.edu.cn
Dr. K. He, Dr. L.-L. Wang, Prof. X.-C. Ma, H.-J. Zhang, Prof. X. Dai, Prof. Z. Fang, Prof. X.-C. Xie, Prof. Q.-K. Xue
Institute of Physics
The Chinese Academy of Sciences
Beijing, 100190 (P. R. China)
Prof. Y. Liu
Department of Physics
The Pennsylvania State University
Pennsylvania, 16802 (USA)
Dr. X.-L. Qi, Prof. S.-C. Zhang
Department of Physics
Stanford University
Stanford, California, 94305-4045 (USA)

DOI: 10.1002/adma.201000368

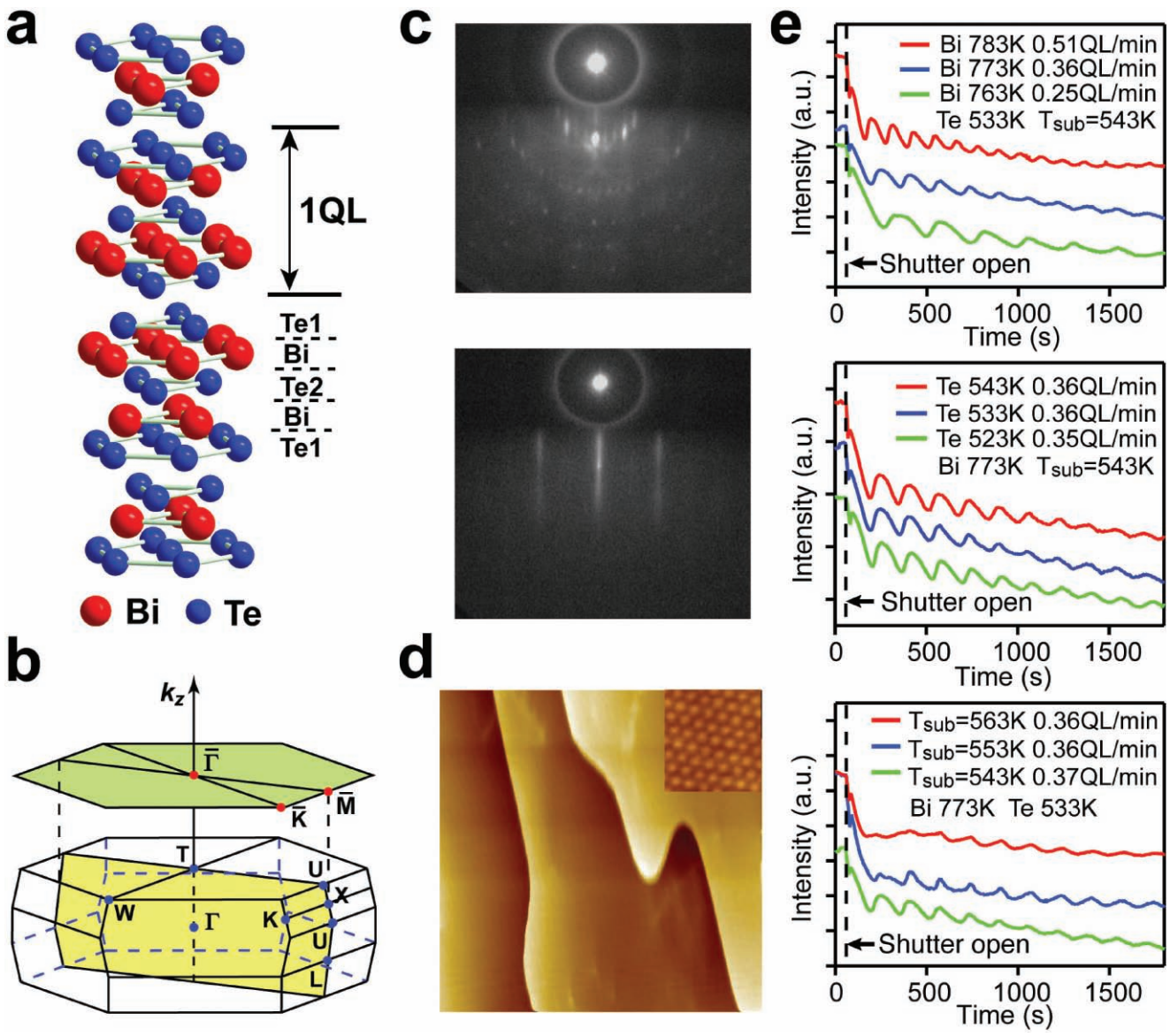

Figure 1. MBE growth of the intrinsic topological insulator of Bi_2Te_3. a) The schematic crystal structure of Bi_2Te_3. b) The bulk and the projected (111) Brillouin zones of Bi_2Te_3. c) The RHEED patterns of the Si(111)-7 × 7 surface and the surface of 4 QL films taken along [11$\bar{2}$] direction. The RHEED pattern shows that the film has a well-defined 1 × 1 symmetry. d) STM image of the 80- nm-thick film grown using the same condition in c). All the steps seen in the image are ~10.17Å in height, corresponding to 1 QL. The image scale is 0.5 μm × 0.5 μm. The insert is an atomically resolved STM image (2.5 nm × 2.5 nm). e) RHEED intensity of the (0, 0) diffraction versus growth time under different flux ratio and temperature. The growth was initiated by opening the Bi shutter. Upper panel: $\theta = 9$ (red), 13 (blue), 19 (green), $T_{si} = 543$ K; Middle panel: $\theta = 20$ (red), 13 (blue), 8 (green), $T_{si} = 543$ K; Lower panel: $\theta = 13$, $T_{si} = 563$ K (red), 553 K (blue), and 543 K (green).

ARPES measurements reveal that the as-grown Bi_2Te_3 films all exhibit the characteristic intrinsic topological feature: E_F lies in between the bulk CBM and the bulk VBM and thus only crosses the metallic surface state. By thickness-dependent band structure measurement, we show that the single-Dirac-cone surface state forms at a thickness of 2 quintuple layers (2 QL), which agrees well with our first principle calculations.

To establish the optimal MBE growth conditions, we start with an analysis of the rhombohedral crystal structure of Bi_2Te_3. As schematically shown in **Figure 1a**, along the [111] crystallographic direction, the unit cell contains five atomic layers with a stacking sequence of Te(1)-Bi-Te(2)-Bi-Te(1), forming a unique QL. The lattice constant along this direction is 10.17Å, while that on the *a-b* (111) plane is 4.38Å. The bulk and the projected (111) Brillouin zones are shown in Figure 1b. The QL is terminated by a Te(1) atomic layer in both sides. The interaction between two adjacent QLs is of the van der Waals type, which is much weaker than that between two atomic layers within a QL.[4] As a result, the cleaved surfaces from a bulk crystal are always Te-terminated and have an unreconstructed (1 × 1)-Te structure.[4,5,18–20] Inspired by the well-established layer-by-layer growth of GaAs with As_4 molecular beam, where the

growth unit is always a Ga-As bilayer along [001] direction,[24] we anticipate that an ideal MBE growth of Bi_2Te_3 with Te_2 molecular beam should proceed under Te-rich conditions and in unit of a QL along the [111] direction.

The optimization of our MBE growth of Bi_2Te_3 involves a set of growth experiments under different Te_2/Bi flux ratios (θ) and substrate temperatures (T_{Si}). It was found that the intrinsic insulator could readily be achieved under Te-rich condition (θ = 8–20) and when the criterion of $T_{Bi} > T_{Si} \geq T_{Te}$ is satisfied. Here, T_{Bi} and T_{Te} are the temperatures of Bi and Te Knudsen cells, which were used to precisely control the deposition flux (thus the ratio) of Bi and Te. The resulting growth rate is typically ~1/3 QL per minute. In Figure 1c, we show the RHEED patterns of the initial Si(111)-7 × 7 surface (upper panel) and the Bi_2Te_3 film with a thickness of 4 QL (lower panel). The electron beam incidence is along [11$\bar{2}$] ($\bar{\Gamma} - \bar{M}$) direction. The sharp streaky pattern as seen in the lower panel indicates that the film has an atomically flat surface morphology. If the surface is rough, the spots rather than streaks will be observed in the RHEED pattern, because three-dimensional diffraction occurs when the grazing incident electrons penetrate through the islands on a rough surface. A typical large-scale STM image of a 80-nm-thick film grown under the same condition is shown in Figure 1d. The atomically flat morphology is immediately evident. The 1 × 1 RHEED pattern, as well as the high resolution STM image with a well-defined 1 × 1 symmetry (see the insert of Figure 1d), reveals that the growing front surface during and after deposition is the Te-terminated Bi_2Te_3(111)-(1 × 1) surface,[18–20] the same as that obtained by cleaving bulk crystals.[5,6] The steps shown in Figure 1d are all 10.17 Å in height, corresponding to 1 QL. As expected, the growth on Si(111) proceeds along the [111] crystallographic direction.

Figure 1e shows the intensity evolution of the (0, 0) diffraction (the central streak) versus growth time under various Te_2/Bi flux ratios and substrate temperatures (T_{Si}). In all nine sets of growth parameters depicted in Figure 1e, there is a persistent RHEED intensity oscillation, which is characteristic of layer-by-layer growth. One period of oscillation corresponds to deposition of a quintuple layer of Bi_2Te_3. In this sense, the growth is better described as QL-by-QL growth. To further demonstrate this, in some runs of our experiment we intentionally interrupted the growth when 1/4 QL had been deposited. The STM images from as-deposited surface show the formation of 2D islands on the flat terraces, and all with a height of 1 QL. This confirms that the growth unit is 1 QL.

Another important observation in growth dynamics is that the growth rate is only dependent on the Bi flux under our growth conditions. As shown in the upper panel of Figure 1e, the growth rate increases by a factor of 2.04 when the Bi cell temperature is increased from 763 K to 783 K. This temperature change corresponds to a change of the Bi beam equivalent pressure by a similar factor of 2.08. On the other hand, there is basically no change in growth rate even with a change of the Te beam equivalent pressure by a factor of 2.65, when T_{Te} is increased from 523 K to 543K. We also found that if only the Te cell shutter is open so that only the Te beam is exposed to the substrate, the Te-terminated 1 × 1 RHEED pattern remains unchanged. It implies that under the condition of $T_{Si} \geq T_{Te}$, the Te_2 molecular beam does not stick to the 1 × 1-Te surface and the film does not grow without simultaneous supply of the Bi atomic beam. This is important since it sets the lower limit of growth temperature for possible stoichiometric deposition. Below this limit, the Te atoms may no longer desorb from the 1 × 1-Te surface, leading to a situation similar to that in methods such as codeposition[23] or bulk crystal growth.[5,6] The unique Te-rich growth dynamics and the criterion of $T_{Bi} > T_{Si} \geq T_{Te}$ observed here are closely analogous to the well-established GaAs MBE growth,[24] confirming our initial hypothesis. Realizing that the only equilibrium phase of BiTe alloys is Bi_2Te_3 when $\theta \geq 3/2$,[25] which is always satisfied here (θ = 8–20), one easily understands why the growth of Bi_2Te_3 is strictly stoichiometric. This feature represents a fundamental difference between our method and those used in Refs.[5,6] and Ref.[23].

To illustrate the quality of the films, we carried out ARPES measurements. **Figure 2** shows the band structure of the 80-nm-thick Bi_2Te_3 films taken along the $\bar{\Gamma} - \bar{M}$ direction.

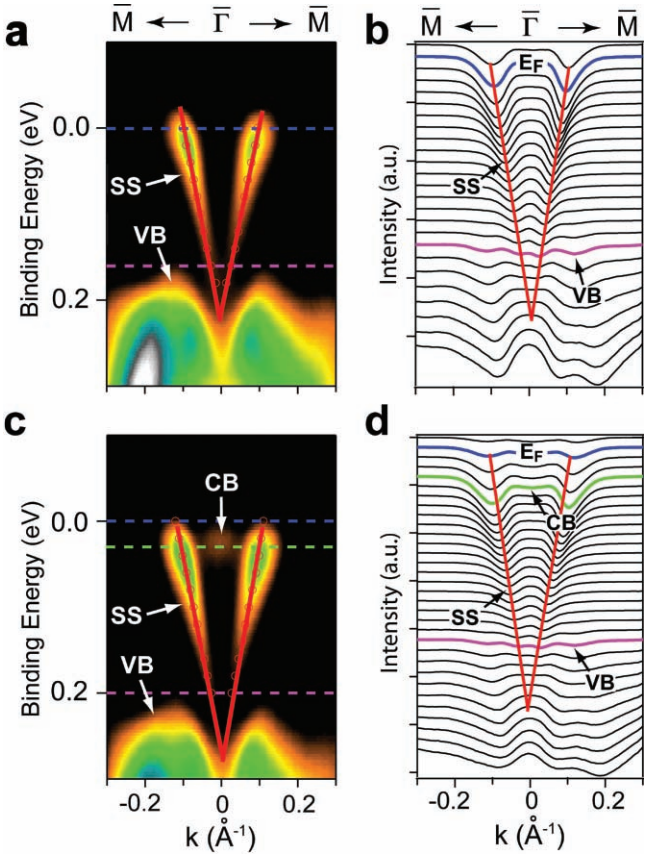

Figure 2. Dirac-like band dispersion near the Γ point in the bulk Brillouin zone of the intrinsic topological insulator Bi_2Te_3 film. The film has a thickness of 80 nm (Figure 1d). a) ARPES intensity map of the film taken right the growth of the film. b) Momentum distribution curves corresponding to the intensity map in a). c) ARPES intensity map of the film after continuous exposure of the photons for two hours. d) Momentum distribution curves corresponding to the intensity map in c). The surface states, valence band and conduction band of the bulk states are denoted SS, VB and CB, respectively. In b) and d), E_F, top of VB and bottom of CB are indicated by the blue, pink curve and green curve, respectively. The momentum distribution curves were measured at an interval of 10 meV. The red lines are guides to the eye for SS in the momentum distribution curves.

The film was grown with a Te_2/Bi flux ratio of 13 at a substrate temperature of 543 K. Besides the broad "M"-shape valence band (VB) at the bottom, a linear band dispersion representing the massless Dirac-like surface states (SS) is clearly seen in Figure 2a. This feature is in agreement with theoretical predictions[4] and recent ARPES measurements on the cleaved (111) surface of the bulk crystal.[5] Most importantly, the bulk conduction bands (CBs) observed in the undoped Bi_2Te_3[5,6] crystals are completely absent at E_F, indicating that the as-grown films without doping are indeed an intrinsic topological insulator. Furthermore, the Bi_2Te_3 films are very stable in the UHV chamber. The ARPES spectra were obtained within 30 minutes after the preparation of the films, and no distinctive change was observed in the ARPES spectra even after 72 hours. In comparison, for the bulk crystal doped with 0.67% Sn, the Fermi level shows an aging effect on the time scale of hours.[5]

When the samples were continuously exposed to the photon beam for two hours, the Fermi level is observed to rise, as shown in Figure 2c. The energy lift as estimated from the VB top is 50 meV. As a result, the bottom of the bulk CB is now located at 30 meV below E_F. The effect is shown more clearly in the momentum distribution curves (Figure 2b and 2d). The lift enables us to estimate the energy gap, which is 170 meV (Figure 2d) and consistent with both theory[4] and another ARPES experiment (165 meV).[4,5] Interestingly, if the sample is electrically grounded or warmed up to room temperature, the Fermi level falls back and the band structure shown in Figure 2a is recovered. We conjecture that the lift is most likely due to optical doping induced charge accumulation.[26] The Fermi velocity along the $\overline{\Gamma}-\overline{M}$ direction from linear fitting (the red lines in Figure 2a) is 3.32×10^5 m/s, which agrees well with the measurement on bulk materials (3.87×10^5 m/s),[5] as well as the first-principles calculation (3.5×10^5 m/s).[4]

Next, we study the thickness dependence of the topological features. In **Figure 3**, we show the evolution of band structure of the Bi_2Te_3 films with a thickness from 1 QL to 5 QL. For the 1 QL film (Figure 3a), there is a nearly parabolic free-electron-like band crossing the Fermi level and a gap (~0.5 eV) between

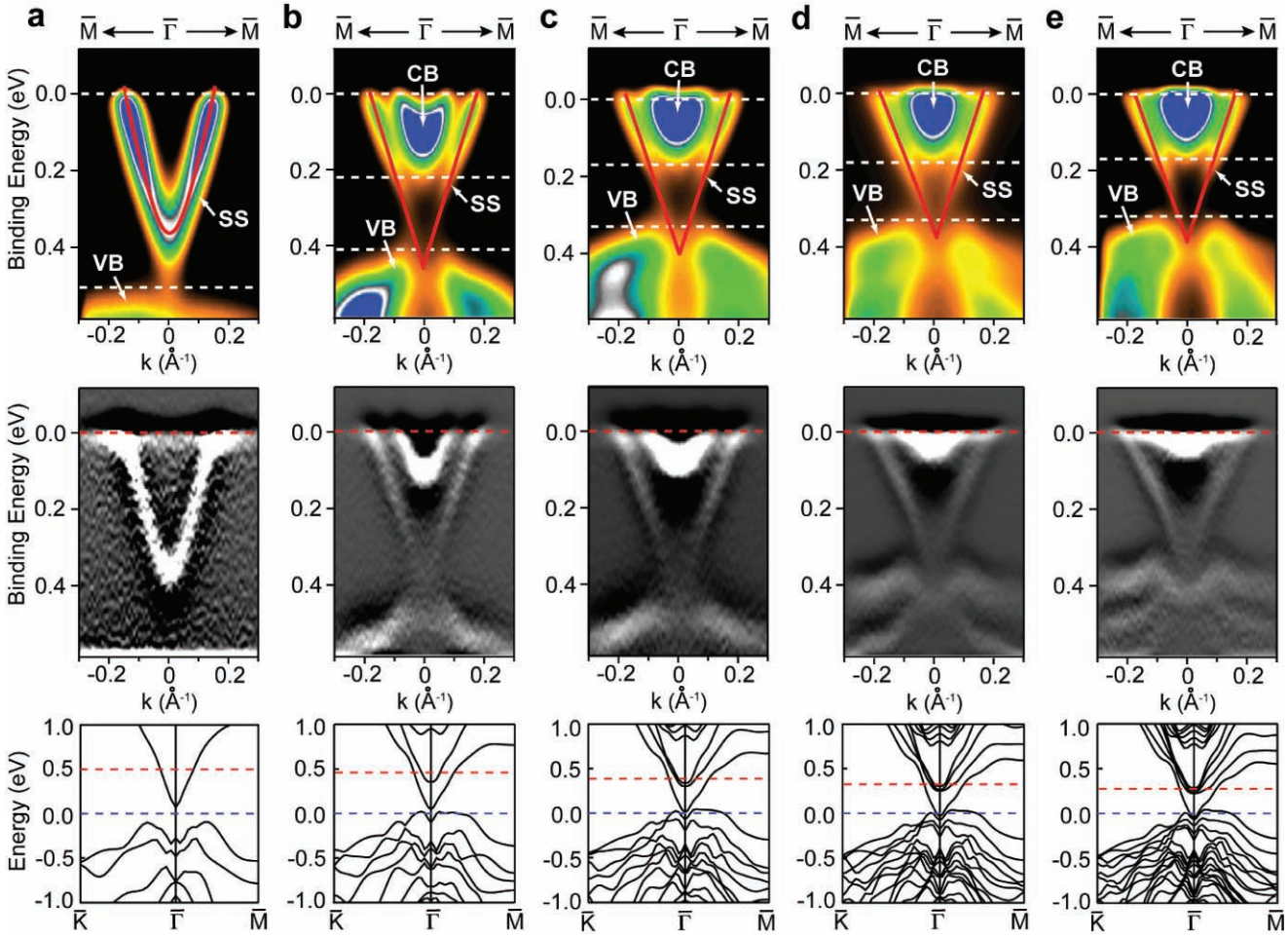

Figure 3. Band structure of ultrathin films of Bi_2Te_3. a) 1 QL. b) 2 QL. c) 3 QL. d) 4 QL. e) 5 QL. All the spectra were taken along the $\overline{\Gamma}-\overline{M}$ direction. Upper panels: ARPES intensity maps; Middle panels: differential ARPES intensity maps; Lower panels: band structures from first-principles calculations. If the Fermi level (blue dashed line) in the calculated band structure (lower panels) is shifted to higher energy (red dashed line), the major features seen in the middle panels are well reproduced.

CB and VB. The topological features start to appear in the 2 QL film, as shown in Figure 3b. Except for an intense and broad bulk electron pocket on the top, the overall band structure is very similar to that of the intrinsic films shown in Figure 2a. To understand the thickness-dependent electronic structure, we carried out first-principles calculations and found excellent agreement between our experiment and theory (lower panels of Figure 3). The surface state decay length is calculated to be about 1 nm based on density functional theory.[27] Therefore, for the 1 QL film, the coupling between top and bottom surfaces is strong enough to open up a whole insulating gap. Starting from the 2 QL film, the inter-surface coupling becomes progressively weaker, and the topological features are recovered.

With increasing thickness, the Fermi level moves toward the bulk gap. The bulk CB is considerably smaller for the 5 QL film. This trend is more clearly revealed by the differential spectra maps (the middle panels of Figure 3). These results demonstrate that both quality and stoichiometry of the film become better as the film grows thick, which is also confirmed by the corresponding STM images. When two surface layers couple to each other in an ultrathin film, a hybridization gap is generally opened up. In this case, there is no clear way to define the concept of the 3D topological insulator. However, the hybridization gap of the 2D film can itself be topologically non-trivial, leading to topologically protected edge states, similar to the case of the HgTe quantum well.[12,13] The layer-by-layer MBE growth of Bi_2Te_3 film enables us to investigate this question with fabricated devices.

To conclude, we have established the Te-rich growth dynamics and criterion for preparing high quality topological films of Bi_2Te_3 by standard MBE technique. The information can apply to MBE growth of other topological materials such as Bi_2Se_3[27] and Sb_2Te_3[4] and on other substrates. Recently, Landau levels were observed in our MBE-grown Bi_2Se_3 films, which implies that the mobility of our films is in order of 10^3 $cm^2/V{\cdot}s$ and thus demonstrates the superior quality of MBE grown TI films.[28] Our MBE-grown Bi_2Te_3 films not only reveal the intrinsic topological surface states in the cleanest manner reported so far, but also pave the road for future device applications involving topological insulators. The unique topological and thermoelectric properties of MBE-grown Bi_2Te_3 make it a strong candidate as a core component in multifunctional heterostructures for quantum computation, spintronics, and local chip cooling.

Experimental Section

Our experiments were performed in an ultrahigh vacuum system that houses an MBE growth chamber, a low temperature scanning tunneling microscope (Omicron) and an angle resolved photoemission spectrometer (GAMMADATA SCIENTA). The base pressure of the system is better than 5×10^{-11} Torr. Si(111)-7 × 7 substrates were cleaned by standard multi-cycle flashing process.[29] RHEED patterns were used to calibrate the in-plane lattice constant of the Bi_2Te_3 films with respect to the Si(111)-7 × 7 surface, while the RHEED intensity of the (0,0) diffraction recorded by a CCD camera was used to measure the growth dynamics. The STM images were acquired at 77K using chemically etched polycrystalline W tips. The ARPES spectra were collected with a R4000 analyzer and a VUV 5000 UV source with a monochrometer. The He I (21.218 eV) resonant line was used to excite photoelectrons. The energy resolution and angular resolution of the analyzer were set at 10 meV and 0.2°, respectively.

Acknowledgements

We would like to thank S. Q. Shen, Y. Ran and L. He for helpful discussions. The work in Beijing is supported by NSFC and the National Basic Research Program from MOST of China. The work at Stanford is supported by the Department of Energy, Office of Basic Energy Sciences, Division of Materials Sciences and Engineering, under contract DE-AC02-76SF00515. Y.L. is supported by DOD ARO under W911NF-07-1-0182, DOE under DE-FG02-04ER46159, and NSFC under 10628408.

Received: February 1, 2010
Published online: July 20, 2010

[1] F. Xiao, C. Hangarter, B. Yoo, Y. Rheem, K.-H. Lee, N. V. Myung, *Electrochim. Acta* **2008**, *53*, 8103.
[2] T. M. Tritt, *Science* **1999**, *283*, 804.
[3] C. B. Saiterthwaite, R. W. Ure Jr., *Phys. Rev.* **1957**, *108*, 1164.
[4] H. J. Zhang, C.-X. Liu, X.-L. Qi, X. Dai, Z. Fang, S.-C. Zhang, *Nat. Phys.* **2009**, *5*, 438.
[5] Y. L. Chen, J. G. Analytis, J.-H. Chu, Z. K. Liu, S.-K. Mo, X. L. Qi, H. J. Zhang, D. H. Lu, X. Dai, Z. Fang, S.-C. Zhang, I. R. Fisher, Z. Hussain, Z.-X. Shen, *Science* **2009**, *325*, 178.
[6] D. Hsieh, Y. Xia, D. Qian, L. Wray, J. H. Dil, F. Meier, J. Osterwalder, L. Patthey, J. G. Checkelsky, N. P. Ong, A. V. Fedorov, H. Lin, A. Bansil, D. Grauer, Y. S. Hor, R. J. Cava, M. Z. Hasan, *Nature* **2009**, *460*, 1101; D. Hsieh, Y. Xia, D. Qian, L. Wray, F. Meier, J. H. Dil, J. Osterwalder, L. Patthey, A. V. Fedorov, H. Lin, A. Bansil, D. Grauer, Y. S. Hor, R. J. Cava, M. Z. Hasan, *Phys. Rev. Lett.* **2009**, *103*, 146401.
[7] X. L. Qi, T. Hughes, S.-C. Zhang, *Phys. Rev. B* **2008**, *78*, 195424.
[8] S.-C. Zhang, *Physics* **2008**, *1*, 6.
[9] X.-L. Qi, R. Li, J. Zang, S.-C. Zhang, *Science* **2009**, *323*, 1184.
[10] Q. Liu, C.-X. Liu, C. Xu, X.-L. Qi, S.-C. Zhang, *Phys. Rev. Lett.* **2009**, *102*, 156603.
[11] Y. Xia, D. Qian, D. Hsieh, L. Wray, A. Pal, H. Lin, A. Bansil, D. Grauer, Y. S. Hor, R. J. Cava, M. Z. Hasan, *Nat. Phys.* **2009**, *5*, 398.
[12] B. A. Bernevig, T. L. Hughes, S.-C. Zhang, *Science* **2006**, *314*, 1757.
[13] M. König, S. Wiedmann, C. Brüne, A Roth, H. Buhmann, L. W. Molenkamp, X.-L. Qi, S.-C. Zhang, *Science* **2007**, *318*, 766.
[14] L. Fu, C. L. Kane, E. J. Mele, *Phys. Rev. Lett.* **2007**, *98*, 106803.
[15] J. E. Moore, L. Balents, *Phys. Rev. B* **2007**, *75*, 121306.
[16] D. Hsieh, D. Qian, L. Wray, Y. Xia, Y. S. Hor, R. J. Cava, M. Z. Hasan, *Nature* **2008**, *452*, 970.
[17] D. Hsieh, Y. Xia, L. Wray, D. Qian, A. Pal, J. H. Dil, J. Osterwalder, F. Meier, G. Bihlmayer, C. L. Kane, Y. S. Hor, R. J. Cava, M. Z. Hasan, *Science* **2009**, *323*, 919.
[18] Y. S. Hor, A. Richardella, P. Roushan, Y. Xia, J. G. Checkelsky, A. Yazdani, M. Z. Hasan, N. P. Ong, R. J. Cava, *Phys. Rev. B* **2009**, *79*, 195208.
[19] S. Urazhdin, D. Bilc, S. D. Mahanti, S. H. Tessmer, *Phys. Rev. B* **2004**, *69*, 085313.
[20] S. Urazhdin, D. Bilc, S. H. Tessmer, S. D. Mahanti, T. Kyratsi, M. G. Kanatzidis, *Phys. Rev. B* **2002**, *66*, 161306.
[21] R. Venkatasubramanian, E. Siivola, T. Colpitts, B. O'Quinn, *Nature* **2001**, *413*, 597.
[22] Y. Iwata, H. Kobayashi, S. Kikuchi, E. Hatta, K. Mukasa, *J. Crys. Growth* **1999**, *203*, 125.
[23] G. Zhang, H. Qin, J. Teng, J. Guo, Q. Guo, X. Dai, Z. Fang, K. Wu, *Appl. Phys. Lett.* **2009**, *95*, 053114.

[24] In a standard MBE growth of GaAs(001) films under As-rich condition (the As_4/Ga ratio is usually set in a range of 30 to 60), the growing front surface remains the stable As-terminated 2×4 reconstruction, which is similar to the Te-terminated 1×1 structure in the present case. Under the condition of $T_{Ga} > T_{substrate} > T_{As}$, the GaAs films grow only when the Ga beam is exposed to the substrate. See Q. K. Xue, T. Hashizume, T. Sakurai, *Prog. Surf. Sci.* **1997**, *56*, 1.

[25] H. Okamoto, L. E. Tanner, *Bi-Te (Bismuth-Tellurium) Phase Diagram*, ASM, **1986**.

[26] Y. Terada, S. Yoshida, A. Okubo, K. Kanazawa, M. Xu, O. Takeuchi, H. Shigekawa, *Nano Lett.* **2008**, *8*, 3577.

[27] W. Zhang, R. Yu, H. J. Zhang, X. Dai, Z. Fang, arXiv:1003.5082.

[28] P. Cheng, C. L. Song, T. Zhang, Y. Y. Zhang, J. F. Jia, J. Wang, Y. Y. Wang, B. F. Zhu, X. Chen, X. C. Ma, K. He, L. L. Wang, X. Dai, Z. Fang, X. C. Xie, X. L. Qi, C. X. Liu, Q. K. Xue, S. C. Zhang, arXiv:1001.3220.

[29] J.-L. Li, J.-F. Jia, X.-J. Liang, X. Liu, J.-Z. Wang, Q.-K. Xue, Z.-Q. Li, J. S. Tse, Z. Zhang, S. B. Zhang, *Phys. Rev. Lett.* **2002**, *88*, 066101.